A subgrid-scale model based on singular values for LES in complex geometries

By H. Baya Toda†, O. Cabrit‡, G. Balarac¶, S. Bose, J. Lee‖, H. Choi‖ AND F. Nicoud ††

An eddy-viscosity based, subgrid-scale model for Large Eddy Simulations is derived from the analysis of the singular values of the resolved velocity gradient tensor. It is shown that the proposed σ-model has the property to automatically vanish as soon as the resolved field is two-dimensional, including the pure shear and solid rotation cases. In addition, the model generates no subgrid-scale viscosity when the resolved scales are in pure axisymmetric or isotropic contraction/expansion. At last, it has the appropriate cubic behavior in the vicinity of solid boundaries without requiring any ad-hoc treatment. Results obtained for different physical configurations (isotropic turbulence, channel flows, and periodic jet) are presented to illustrate the potential of the model. A dynamic version based on a volume averaged procedure is also proposed.

1. Introduction

When dealing with Large Eddy Simulations (LES), the eddy-viscosity assumption is by far the most used because it reduces the modeling effort considerably. In this view, the subgrid-scale (SGS) tensor is written as $\tau_{ij}^{\mathrm{SGS}} - \frac{1}{3}\tau_{kk}^{\mathrm{SGS}}\delta_{ij} = 2\nu_{\mathrm{SGS}}S_{ij}$, where $S_{ij} = \frac{1}{2}\left(g_{ij} + g_{ji}\right)$ and $g_{ij} = \partial u_i/\partial x_j$ is the velocity gradient tensor of the resolved scales. Note that the (implicit) filter $\bar{\cdot}$ is omitted throughout this paper for simplicity. From a simple dimensional analysis, it is natural to model the subgrid-scale viscosity as

$$\nu_{\mathrm{SGS}} = \left(C_m\Delta\right)^2 \mathcal{D}_m(\mathbf{u}), \tag{1.1}$$

where C_m is the model constant, Δ is the subgrid characteristic length scale (in practice the size of the mesh), and $\mathcal{D}_m$ is a differential operator associated with the model, homogeneous to a frequency and acting on the resolved velocity field $\mathbf{u} = (u_i)$. The most classical operator is by far the strain rate; this leads to the Smagorinsky (1963) model for which $\mathcal{D}_m = \mathcal{D}_s = \sqrt{2S_{ij}S_{ij}}$ and $C_m = C_s \approx 0.18$. This operator is known for not vanishing in near-wall regions. In the past, this major drawback (not the only one of the Smagorinsky operator) motivated the use of damping functions (Moin & Kim, 1982) and the development of the dynamic procedure by Germano *et al.* (1991). It is actually possible to overcome this weakness by using advanced models that naturally vanish in pure shear regions such as the WALE (Wall Adapting Local Eddy viscosity) and Vreman models (Vreman, 2004). However, all the models based on the eddy-viscosity assumption, Eq. 1.1, share the drawback that the model constant C_m must be adapted to the mesh refinement so that the proper amount of energy is drained from the resolved

† IFP Energie Nouvelles
‡ CERFACS
¶ LEGI
‖ Seoul National University
†† CNRS UMR 5149. Corr. author: franck.nicoud@univ-montp2.fr

scales. This issue is well addressed by the introduction of a dynamic procedure that can automatically adapt the model constant. In this view, the model constant C_m can be computed resorting to a least squares approach proposed by Lilly (1992),

$$(C_m\Delta)^2 = -\frac{L_{ij}M_{ij}}{2M_{ij}M_{ij}}, \tag{1.2}$$

where $L_{ij} = \widetilde{u_i\,u_j} - \widetilde{u}_i\,\widetilde{u}_j$ is the (modified) Leonard term based on the grid-based filter (which is omitted for clarity, $\overline{u_i} = u_i$) and test filter $\widetilde{\cdot}$. In addition, M_{ij} is directly related to the differential operator and the eddy-viscosity model is based on

$$M_{ij} = \frac{\widetilde{\Delta}^2}{\Delta^2}\widetilde{\mathcal{D}_m}\widetilde{S_{ij}} \;-\; \widetilde{\mathcal{D}_m\,S_{ij}},$$

where $\widetilde{\Delta}$ stands for the test filter width. Unfortunately, the original dynamic procedure most often requires some averaging in order to reduce the constant variability over space and time. Several improved versions of the dynamic Smagorinsky model were proposed in order to make it more robust and suitable for complex configurations where no homogeneous directions are present (Ghosal, 1995; Meneveau *et al.*, 1996). Still, the common practice when dealing with complex geometries is to apply the least mean square formula over a small volume surrounding the current grid point and to clip the remaining negative values of the dynamically computed constant. This means replacing Eq. 1.2 by

$$(C_m\Delta)^2 = \max\left[-\frac{\langle L_{ij}M_{ij}\rangle_{\mathrm{loc}}}{2\,\langle M_{ij}M_{ij}\rangle_{\mathrm{loc}}}, 0\right], \tag{1.3}$$

where $\langle\cdot\rangle_{\mathrm{loc}}$ stands for an integral taken over a small volume (typically a few grid cells) surrounding the current grid point. Note that the model constant then depends on both space and time.

The main motivation of the local dynamic procedure was to adapt the constant to compensate the non-vanishing behavior of the Smagorinsky model in near-wall regions. Recently, Ghorbaniasl & Lacor (2008) proposed to extend the dynamic procedure to the WALE model. However, Baya Toda *et al.* (2010) reported that the combination of the classical dynamic procedure with any SGS model that has the proper near-wall cubic behavior leads to a paradox: the underlying differential operator rapidly goes to zero near solid boundaries, which favors unstable computations. For the sake of robustness while keeping an adaptation of the model coefficient to the grid resolution and numerical errors, two concepts of global dynamic procedure emerged from the properties of the Vreman model. The first one is based on the global equilibrium hypothesis (da Silva & Metais, 2002) and was proposed by Park *et al.* (2006) and was later improved by You & Moin (2007). The second one, based on the Germano identity, was also proposed by Park et al. (2006) and was proven to be better suited for transient flows (Lee *et al.*, 2010). This global dynamic procedure amounts to change Eq. 1.3 to

$$(C_m\Delta)^2 = -\frac{\langle L_{ij}M_{ij}\rangle_{\mathrm{dom}}}{2\,\langle M_{ij}M_{ij}\rangle_{\mathrm{dom}}}, \tag{1.4}$$

where $\langle\cdot\rangle_{\mathrm{dom}}$ stands for an averaging over the whole computational domain; the model constant is then uniform over space by construction. It has the advantage of producing mostly positive values for the dynamic constant, thus avoiding the clipping issue. The price to pay is that the differential operator $\mathcal{D}_m$ must behave appropriately in basic flow configurations because no compensation from the dynamic procedure can be ex-

pected (the constant of the model is uniform over space). For example, such formulation is not expected to provide good results if applied to the Smagorinsky model since the eddy-viscosity would then not vanish near solid walls. The differential operators used in the WALE and Vreman models are not very appropriate either. For example, it can be shown analytically that the latter is linear with respect to the distance to solid boundaries instead of having a cubic behavior in near-wall regions. Also, they both produce non zero eddy-viscosity in simple flow configurations such as solid rotation, and more generally two-dimensional and/or two-component (2C) flows, where no subgrid scale activity is expected to occur. Indeed, although two-dimensional turbulence has been evidenced experimentally and numerically (Lesieur, 2008), it is a phenomenon of fundamental interest that "might thus be viewed as just a toy model" (Frisch, 1995). Given that two- and three-dimensional turbulence are fundamentally different because of the absence of the vortex-stretching term in the former, it seems appropriate to make sure that any SGS model for three-dimensional turbulence switches off in the two-dimensional case. The alternative would be to switch to a SGS model appropriate for two-dimensional turbulence. Still, given the very little probability that a three-dimensional computation of a two-dimensional turbulent flow remains two-dimensional without any external action to maintain its two-dimensionality, this choice was not pursued. At the end, the main objective of this paper is to define and test a new static model for three-dimensional flows with better properties than the existing formulations. The analytical formulation is provided in section 2, numerical results are discussed in section 3.

2. A singular values-based model

Several properties are desirable for an improved differential operator, although establishing a definite list of such properties would be a very difficult task. Similar to the WALE and Vreman models, the operator should tend to zero in near-wall regions in order to mimic the turbulence damping due to the no-slip condition. It can be shown that the turbulent stress, thus the eddy-viscosity and the differential operator, would decay as the distance to the solid boundary to the third power (Chapman & Kuhn, 1986) (**Property P1**). At the same time, it would vanish in the case of a flow in solid rotation, like the Smagorinsky model, and in the case of a pure shear, like the WALE and Vreman models. More generally, the improved differential operator should be zero for any two-dimensional flow (**Property P2**). Indeed, such a situation for the resolved scales is not compatible with a subgrid-scale activity, which is presumably three-dimensional. The same reasoning leads to the conclusion that the SGS viscosity should be zero in the case where the resolved scales are either in pure axisymmetric or isotropic contraction/expansion (**Property P3**). The former case corresponds to the situation of a laminar round jet impinging on a solid plate for which turbulent effect should indeed not be present. The latter is representative of the velocity field near an acoustic monopole or a spherical premixed flame, which again are not phenomena of turbulent nature.

Analyzing the spectral content of the velocity gradient tensor proves to be a proper framework to investigate how these properties can be met by a single differential operator. Note, however, that the eigenvalues of $\mathbf{g}$ can be complex-valued in number of flow configurations (in the case of a solid rotation, for example). One way to avoid this difficulty is to consider the strain rate tensor instead of $\mathbf{g}$. In this case, the three eigenvalues are real-valued, although their sign is not known a priori. This route is explored in another paper in this volume (Verstappen & Bose, 2010). In the present study, one relies on

the singular value decomposition of $\mathbf{g}$ to build an improved differential operator for the SGS eddy viscosity. Specifically, let us introduce $\sigma_1 \geq \sigma_2 \geq \sigma_3 \geq 0$, the three singular values of $\mathbf{g} = (g_{ij})$. By definition, these values are always positive and equal the square root of the eigenvalues of the matrix $\mathbf{G} = \mathbf{g}^t\mathbf{g}$ (which are always positive because $\mathbf{G}$ is symmetric semi-definite positive). The smallest singular value, σ_3, is null if and only if one row or column of $\mathbf{g}$ is zero up to a rotation of the coordinate system. In other words, $\sigma_3 = 0$ is a marker for two-dimensional and/or 2C flows, and any operator proportional to this singular value would meet property **P2**. Similarly, the knowledge of the singular values of $\mathbf{g}$ helps to detect the case where the resolved velocity field is in axisymmetric contraction or expansion. Indeed, an appropriate rotation of the coordinate system then makes the velocity gradient tensor diagonal:

$$\mathbf{g} = \mathrm{diag}\,(\beta, -\alpha, -\alpha), \tag{2.1}$$

where α is positive for a contraction and negative for an expansion. Depending on the relative values of the parameters α and β, the singular values of $\mathbf{g}$ read either $\sigma_1 = |\beta| > \sigma_2 = \sigma_3 = |\alpha|$ or $\sigma_3 = |\beta| < \sigma_1 = \sigma_2 = |\alpha|$. In other words, the marker for such flow situations is either $\sigma_2 = \sigma_3$ or $\sigma_1 = \sigma_2$. Also a isotropic contraction/expansion corresponds to $\sigma_1 = \sigma_2 = \sigma_3$, thus any differential operator proportional to $(\sigma_1 - \sigma_2)(\sigma_2 - \sigma_3)$ would meet property **P3**. Note that the divergence-free assumption was not made to obtain the above results (β not necessary equal to 2α).

From the above analysis, a differential operator proportional to $\sigma_3(\sigma_1 - \sigma_2)(\sigma_2 - \sigma_3)$ would meet both properties **P2** and **P3**. By analyzing the asymptotic behavior of the singular values in the vicinity of a solid boundary, it is actually possible to show that

$$\sigma_1 = O(y^0) \quad ; \quad \sigma_2 = O(y^1) \quad ; \quad \sigma_3 = O(y^2). \tag{2.2}$$

The algebra that leads to this result is not given in this report for the sake of simplicity. Eqs. 2.2 indicate that the product $\sigma_3(\sigma_1 - \sigma_2)(\sigma_2 - \sigma_3)$ selected to meet properties **P2** and **P3** is of order $O(y^3)$ near solid boundaries and thus meets property **P1**. The derivation of the differential operator is finished by choosing a scaling factor so that it is a frequency scale. A natural choice is the use the largest singular value σ_1, which is nothing but the norm of $\mathbf{g}$, and which would not change the asymptotic behavior of the ratio. Finally, the proposed SGS model and associated differential operator read

$$\nu_{\mathrm{SGS}} = (C_\sigma \Delta)^2 \mathcal{D}_\sigma \quad ; \quad \mathcal{D}_\sigma = \tfrac{\sigma_3(\sigma_1 - \sigma_2)(\sigma_2 - \sigma_3)}{\sigma_1^2}. \tag{2.3}$$

This model will be referred to as the σ-model in the remaining of this paper.

Table 1 summarizes the properties of different differential operators and associated models. Contrary to what is often mentioned, the asymptotic behavior of the Vreman model is linear in y instead of being cubic. Thus, only the WALE and σ models comply with property **P1**. Note however that the first order behavior of the Vreman model is enough to make it more suitable for wall-bounded flows than the Smagorinsky model for which the eddy-viscosity does not tend to zero because $\mathcal{D}_s = O(y^0)$. Table 1 also shows that the σ-model meets properties **P2**-**P3**, contrary to the other formulations which all fail at some point. It also shares with the three other models the common property that involves only one-point velocity gradients; it is thus easy to implement in any general purpose LES code. The value reported for the model constant C_σ is a rough estimation generated by equating the averaged SGS dissipation obtained by feeding the Smagorinsky model and Eq. 2.3 with a large sample of random velocity gradient tensors. Of course, a more accurate assessment could be done by performing appropriate computations, for

Model	Smagorinsky Smagorinsky (1963)	WALE Nicoud & Ducros (1999)	Vreman Vreman (2004)	σ-model Present
Operator Model constant	$\sqrt{2S_{ij}S_{ij}}$ $C_s \approx 0.18$	Eq. 13 of above ref. $C_w \approx 0.50$	Eq. 35 of above ref. $C_v \approx 0.28$	Eq. 2.3 $C_\sigma \approx 1.5$
Asymptotic **P1**	$O(y^0)$ NO	$O(y^3)$ YES	$O(y)$ NO	$O(y^3)$ YES
Solid rotation Pure shear **P2**	0 1 NO	≈ 0.90 0 NO	≈ 0.71 0 NO	0 0 YES
Axisym Isotropic **P3**	≈ 3.46 ≈ 2.45 NO	≈ 0.15 0 NO	≈ 1.22 1 NO	0 0 YES

TABLE 1. Properties of the SGS models considered. Labels Axisym and Isotropic refer to axisymmetric and isotropic contraction/expansion respectively. The entries below the **P1** row are the values taken by the differential operators when all the velocity derivatives are zero except: Solid rotation: $du_1/dx_2 = -1$ and $du_2/dx_1 = 1$; Pure shear: $du_1/dx_2 = 1$; Axisym: $du_1/dx_1 = \pm 2$, $du_2/dx_2 = \mp 1$, $du_3/dx_3 = \mp 1$; Isotropic: $du_1/dx_1 = \pm 1$, $du_2/dx_2 = \pm 1$, $du_3/dx_3 = \pm 1$

example, of decaying isotropic turbulence cases. This task is not pursued here since the result of any tuning effort would depend on the grid resolution and numerics. Note, however, that the random procedure used to assess C_σ leads to fair estimates of the WALE and Vreman's constant [$C_w \approx 0.63$ and $C_v \approx 0.29$, to be compared with the values recommended by Nicoud & Ducros (1999) and Vreman (2004) and reported in Table 1]. The chosen value $C_\sigma = 1.5$ is thus sufficient to assess the potential of the static σ-model. The proper way to reduce the influence of the selected value for the model coefficient is to use some kind of dynamic procedure able to compensate, at least partly, for the grid resolution and numerical errors. Concerning this topic, a Germano-identity-based global dynamic procedure applied to the σ-model will be presented in section 3.

3. Numerical experiments

The σ-model was implemented in several numerical tools for LES and tested over a variety of academic flow configurations.

• **Solver A**: The general purpose AVBP code was developed at CERFACS and IFP Energies Nouvelles. It is based on a cell-vertex formulation and embeds a set of finite element/ finite volume schemes for unstructured meshes. In the present study a centered Galerkin finite element method (4^{th} order in space) with a 3^{rd} order Runge-Kutta temporal integration is retained for the investigation of two configurations: the decaying isotropic turbulence from the Comte-Bellot & Corsin (CBC) experiment and a turbulent channel flow at Reynolds number $Re_\tau = 395$. These flows were computed with the Dynamic Smagorinsky model and the present static σ-model. The dynamic procedure was applied locally, without averaging over homogeneous directions. Negative values of the

dynamically tuned constant of the Smagorinsky model were clipped to ensure stability (see Eq. 1.3).

- **Solver B**: a finite difference code dedicated to the computation of turbulent channels and developed at the Center for Turbulence Research. It is based on a kinetic energy conserving, 4^{th} order scheme in space as proposed by Morinishi *et al.* (1998). A 3^{rd} order Runge-Kutta scheme is used for the time integration, except for the diffusion terms in the direction normal to the wall that are integrated thanks to an Crank-Nicholson scheme. The divergence-free condition is met by a projection scheme. It was used to compute the turbulent channel flow case at $Re_\tau = 590$ with both the dynamic Smagorinsky model and the present static σ-model. Note that contrary to the implementation used in the general purpose AVBP solver, the dynamic procedure is not applied locally in this case. Instead, the Smagorinsky constant is computed as

$$(C_s\Delta)^2 = -\frac{\langle L_{ij}M_{ij}\rangle_{\text{plane}}}{2\langle M_{ij}M_{ij}\rangle_{\text{plane}}}, \tag{3.1}$$

where $\langle\cdot\rangle_{\text{plane}}$ stands for an integral taken over homogeneous planes parallel to the walls of the channel. This avoids clipping while keeping the favorable dependence of the model constant on the distance to the solid boundaries.

- **Solver C**: a dealiased spectral code developed at Seoul National University. It is based on a 2^{nd} order semi-implicit scheme for time integration: diffusion terms are treated implicitly using the Crank-Nicolson method, and a 3^{rd} order Runge-Kutta scheme is applied to convection terms. The decaying isotropic turbulence from the Comte-Bellot & Corsin (1971) experiment was computed with a dynamic version of the σ-model. The Germano-based global dynamic procedure (Park *et al.*, 2006; Lee *et al.*, 2010) was used (see Eq. 1.4), meaning that a single-model constant was computed for the whole domain at each iteration. A divergence-free initial field was generated using the re-scaling method proposed by Kang *et al.* (2003).
- **Solver D**: a pseudo-spectral code developed at the LEGI lab in Grenoble, France. With this tool, the viscous terms are treated exactly using a 2^{nd} order explicit Runge-Kutta time-advancement. A classical two-third rule is used for dealiasing the non-linear convection term. This tool was used to compute the case of a periodic plane jet as described in da Silva & Pereira (2008). Several SGS formulations were considered, including the global dynamic σ and Smagorinsky models (both based on the procedure of Eq. 1.4), a local dynamic Smagorinsky model with clipping (see Eq. 1.3), and a planewise dynamic Smagorinsky model without clipping (see Eq. 3.1).

3.1. *Isotropic decaying turbulence*

We first validate the behavior of the σ-model for the simple case of a freely decaying isotropic homogeneous turbulence. The experiment by Comte-Bellot & Corrsin (1971) on decaying turbulence behind a grid is simulated, where the mesh size of the grid turbulence is $M = 5.08$ cm and the free-stream velocity is $U_0 = 10$ m/s. The Taylor micro-scale Reynolds number is $Re_\lambda = u_{rms}\lambda/\nu = 71.6$ at time $tU_0/M = 42$ and decreases to 60.6 at $tU_0/M = 171$. In a reference frame moving with the average flow velocity the problem can be thought of as freely decaying isotropic turbulence. We model this by considering the fluid to be inside a cube-shaped box with periodic boundary conditions. The flow was first computed with the general purpose code AVBP (**Solver A**), where the static σ-model was implemented with $C_\sigma = 1.5$. The grid resolution was 61^3 and Fig. 1 shows that the computed spectra are in fair agreement with the experimental data. The

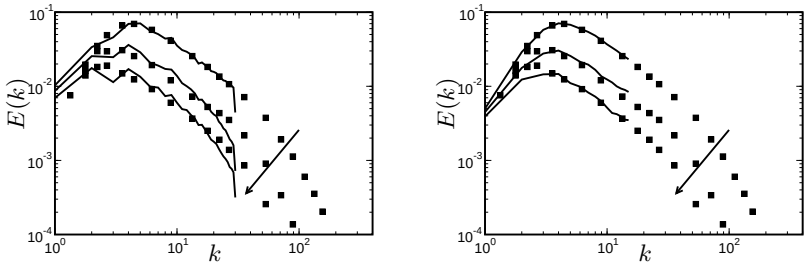

FIGURE 1. Time evolution of energy spectra for freely decaying isotropic turbulence with the σ-model. Symbols are experimental measurements corresponding to the three-dimensionless times $tU_0/M = 42$, 98 and 171. Left: Results from general purpose solver AVBP (**Solver A**) with grid 61^3. Static σ-model. Right: Results from spectral code (**Solver C**) with grid 32^3. Global dynamic σ-model.

biggest differences are obtained for the smallest scales; they are most probably from the large numerical errors that characterize finite volume/finite element methods for large wave numbers. This is confirmed by the results obtained from the spectral code **Solver C** which are essentially in good agreement with the measurements, although the grid is even coarser (32^3). Note that the global dynamic σ-model was used in this case; the constant (homogeneous in space) varied only weakly with time during the simulation with $C_\sigma \approx 1.5 - 1.7$, in close agreement with the value retained from the random procedure (see Table 1).

3.2. *Turbulent Channel flow*

The performance of the static σ-model for wall-bounded flows was investigated by computing LES of turbulent channel flows at friction Reynolds number $Re_\tau = 395$ and 590 with solvers **Solver A** (general purpose) and **Solver B** (channel solver), respectively. In both cases, the computed mean velocity profile is in good agreement with the DNS data from Moser *et al.* (1999), as displayed in Fig. 2. The results are in fact slightly better than what is obtained with the dynamic Smagorinsky model. The same trend is observed when looking at the velocity fluctuations (not shown). The theoretical asymptotic behavior of the σ-model near solid boundaries ($\nu_{\rm SGS} = O(y^3)$) is also well retrieved numerically, as shown in Fig. 3. Note that the amount of SGS eddy-viscosity is not negligible in front of the molecular viscosity, at least in the core region. This reflects the fact that the grid resolution is far from what is required to perform DNSs of the same flows: $\Delta x^+ \approx 48$, Δy^+ in the range 1-17, $\Delta z^+ \approx 10$ for the LES at $R_\tau = 395$ - **Solver A**; $\Delta x^+ \approx 58$, Δy^+ in the range 1-17, $\Delta z^+ \approx 29$ for the LES at $R_\tau = 590$ - **Solver B**. This figure also illustrates that the proper asymptotic behavior is obtained with the dynamic Smagorinsky model only when the plane-wise procedure (Eq. 3.1) is applied, as for the case $R_\tau = 590$ and **Solver B**. Recall that this procedure can be used only for simple cases with homogeneous directions. Conversely, the asymptotic behavior is built in the σ-model's differential operator itself and no specific dynamic procedure/homogeneous directions is required.

3.3. *Turbulent Plane jet*

Further LESs of a periodic planar jet configuration were performed in order to illustrate the potential of the global dynamic σ-model. The spectral code **Solver D** was used. The results from several 64^3 LESs are compared to 256^3 DNS data obtained by running the same spectral code. The configuration is close to the one studied in da Silva & Pereira (2008) except for the jet width-to-initial momentum thickness, which is 20 instead of 35. The

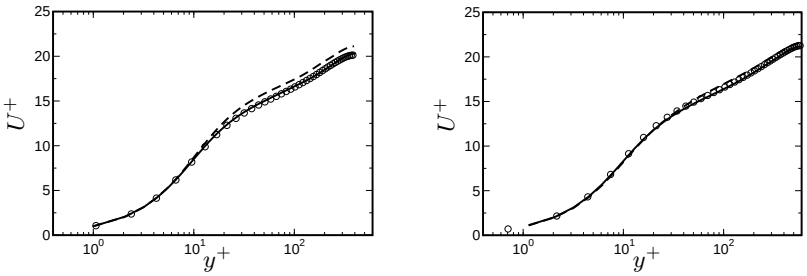

FIGURE 2. Mean velocity profile from the static σ-model (———) and the dynamic Smagorinsky model (- - - -). Symbols correspond to the DNS data of Moser *et al.* (1999). Some symbols of the DNS were removed for clarity. Left: Results from the general purpose solver AVBP (**Solver A**) at $Re_\tau = 395$. Right: Results from the channel code (**Solver B**) at $Re_\tau = 590$.

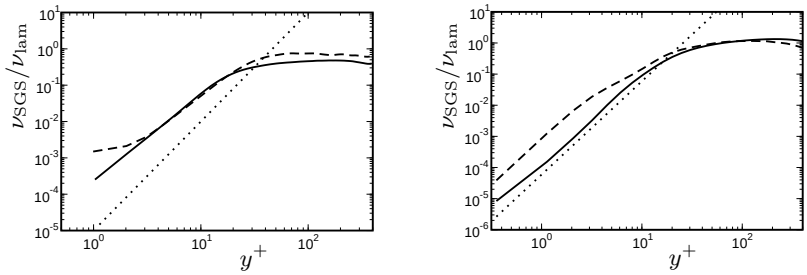

FIGURE 3. Scaled SGS eddy-viscosity from the static σ-model (———) and the dynamic Smagorinsky model (- - - -). The dotted lines correspond to the proper y^3 asymptotic behavior. Left: Results from general purpose solver AVBP (**Solver A**) at $Re_\tau = 395$. Right: Results from the channel code (**Solver B**) at $Re_\tau = 590$.

computational domain is periodic in the three spatial directions and its size is four times the initial jet width. The DNS initial field is generated by super-imposing divergence-free random fluctuations to the mean velocity profile. The LES initial condition is obtained from the DNS data by spectral interpolation. Because periodic conditions are imposed in both the streamwise and spanwise directions, the flow is not statistically steady and the jet keeps growing thicker and thicker as time increases. Figure 4 displays the resolved kinetic energy and SGS eddy-viscosity. from the different LES performed at time 12 h/U where h is the jet width and U is the maximum mean velocity. Note that the profiles are not symmetric because only plane-averaging over the homogeneous directions was applied and the flow is not statistically stationary. Regarding the dynamic Smagorinsky model, the best agreement with the filtered DNS is obtained when the dynamic procedure is applied planewise (see Eq. 3.1). This formulation permits the combination of accuracy (the model constant depends on the position in the plane jet) and robustness (the planar averaging stabilizes the procedure sufficiently to avoid clipping). When the dynamic procedure is applied locally to the Smagorinsky model, Eq. 1.3, a large amount of clipping is required to stabilize the pointwise model constant, and the overall accuracy degrades. On the other hand, when the global procedure, Eq. 1.4, is applied, the model constant is uniform over space and no clipping is required. However, a high level of eddy-viscosity is generated in the mean shear regions because the mean gradient contributes to the strain rate. As a consequence, the resolved scales are over-dissipated and their kinetic energy is under-estimated. Note that the over-estimation of ν_{SGS} does not appear in Fig. 4 because the amount of fluctuation is already way too small at the instant considered.

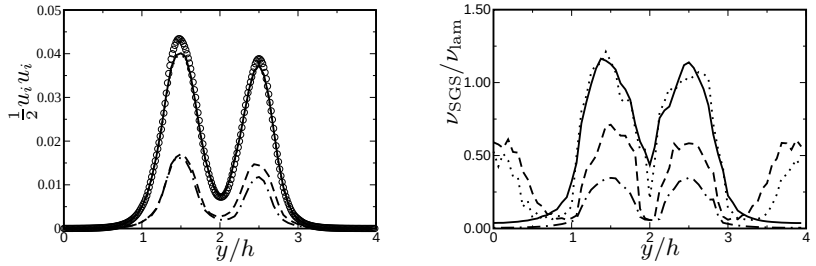

FIGURE 4. LES of a periodic plane jet with a 64^3 grid performed with the spectral code **Solver D**. The global dynamic σ-model (———) at time 12 h/U is compared with the local (– – – –), planewise (·····) and global (—·—) dynamic Smagorinsky models. Left: Resolved kinetic energy. Symbols correspond to the filtered 256^3 DNS. Right: SGS eddy-viscosity scaled by the molecular viscosity.

On the contrary, because the static σ-model produces zero eddy-viscosity for the mean shear associated with the jet, applying the same global dynamic procedure to this model leads to much better results, comparable to the planewise dynamic Smagorinsky model. Note, however, that the global dynamic σ-model can readily be extended to any complex geometry because neither averaging over homogeneous directions nor clipping are required.

4. Conclusions

A differential operator based on the singular values of the velocity gradient tensor is proposed as a basis for an improved SGS eddy-viscosity model. It is shown that the proposed static σ-model generates zero eddy-viscosity for any two-dimensional or 2C flows, as well as for axisymmetric and isotropic situations. It also has the proper cubic behavior in near-wall regions. Owing to its unique properties, this model is well suited for the global dynamic procedure, which adapts the overall coefficient to the grid resolution and numerical errors. The σ-model was implemented in several academic and general purpose CFD codes, under either its static or global dynamic version. The results presented in this report are promising because of the relative ease of implementation. It is anticipated that the σ-model could be useful in the current effort to make LES even more suitable for complex flow configurations.

Hubert Baya Toda gratefully acknowledges support from IFP Energies Nouvelles. CINES and IDRIS from GENCI are acknowledged for giving access to super-computing facilities. The authors also thank Prof P. Moin for fruitful discussions.

REFERENCES

AVBP 2006 Avbp code : www.cerfacs.fr/cfd/avbp_code.php and www.cerfacs.fr/cfd/ cfd-publications.html

BAYA TODA, H., TRUFFIN, K. & NICOUD 2010 Is the dynamic procedure appropriate for all SGS models? In V European Conference on Computational Fluid Dynamics, ECCOMAS (ed. J. C. F. Pereira & A. Sequeira).

CHAPMAN, D. & KUHN, G. 1986 The limiting behavior of turbulence near a wall. *J. Fluid Mech.* **170**, 265–292.

Comte-Bellot, G. & Corrsin, S. 1971 Simple Eulerian time correlation of full- and narrow-band velocity signals in grid generated, 'isotropic' turbulence flows. *J. Fluid Mech.* **48**, 273–337.

Da Silva, C. B. & Metais, O. 2002 On the influence of coherent structures upon interscale interaction in turbulent plane jets. *J. Fluid Mech.* **473**, 103-145.

da Silva, C.; & Pereira, J. 2008 Invariants of the velocity-gradient, rate-of-strain, and rate-of-rotation tensors across the turbulent/nonturbulent interface in jets. *Phys. Fluids* **20**, 055101.

Frisch, U. 1995 Turbulence: The Legacy of A.N. Kolmogorov. *Cambridge University Press*.

Germano, M. 1991 A dynamic subgrid-scale eddy viscosity model. *Phys. Fluids* **3** (7), 1760–1765.

Ghorbaniasl, G. & Lacor, C. 2008 Sensitivity of SGS models and of quality of LES to grid irregularity. In J. Meyers et al. (Eds), Quality and Reliability of Large-Eddy Simulations. Springer Science + Business Media B.V.

Ghosal, S., Lund, T., Moin, P. & Akselvoll, K. 1995 A dynamic localization model for large-eddy simulation of turbulent flows. *J. Fluid Mech.* **286**, 229–255.

Kang H. S., Chester S. and Meneveau C. 2003 Decaying turbulence in an active-grid-generated flow and comparisons with large-eddy simulation *J. Fluid Mech.* **480**, 129.

Lee, J., Choi, H. & Park, N. 2010 Dynamic global model for large eddy simulation of transient flow. *Phys. Fluids* **22**, 075106.

Lesieur, M. 1995 Turbulence in Fluids. *Springer Verlag - 4th Edition*.

Lilly, D. K. 1992 A proposed modification of the Germano subgrid-scale closure method. *Phys. Fluids* **4** (3), 633–635.

Meneveau, C., Lund, T. & Cabot, W. 1996 A lagrangian dynamic subgrid-scale model of turbulence. *J. Fluid Mech.* **319**, 353–385.

Moin, P. & Kim, J. 1982 Numerical investigation of turbulent channel flow. *J. Fluid Mech.* **118**, 341–377.

Morinishi Y., Lund T., Vasilyev O. & Moin P. 1998 Fully conservative higher order finite difference schemes for incompressible flow *J. Comp. Phys.* **143**(1), 90-124.

Moser, R., Kim, J. & Mansour, N. 1999 Direct numerical simulation of turbulent channel flow up to $Re_\tau = 590$. *Phys. Fluids* **11**, 943–945.

Nicoud, F. & Ducros, F. 1999 Subgrid-scale stress modelling based on the square of the velocity gradient. *Flow, Turb. and Combustion* **62** (3), 183–200.

Park, N., Lee, S., Lee, J. & Choi, H. 2006 A dynamic subgrid-scale eddy viscosity model with a global model coefficient. *Phys. Fluids* **18**, 125109.

Smagorinsky, J. 1963 General circulation experiments with the primitive equations: 1. the basic experiment. *Mon. Weather Rev.* **91**, 99–164.

Verstappen, R. & Bose, S. 2010 When does eddy-viscosity damp subfilter scales sufficiently? In Proceedings of the 13th Summer Program of the Center for Turbulence Research.

Vreman, A. 2004 An eddy-viscosity subgrid-scale model for turbulent shear flow: Algebraic theory and applications. *Phys. Fluids* **16** (10), 3670.

You, D. & Moin, P. 2007 A dynamic global-coefficient subgrid-scale eddy-viscosity model for large-eddy simulation in complex geometries. *Phys. Fluids* **19**, 065110/1–8.